ChemPubSoc Europe

DOI: 10.1002/slct.201701755

Chemistry SELECT Full Papers

Sustainable Chemistry

Stoichiometric Control of Electrocatalytic Amorphous Nickel Phosphide to Increase Hydrogen Evolution Reaction Activity and Stability in Acidic Medium

Ruwani N. Wasalat hanthri,[a] Samuel Jeffrey,[a] Naheya Su,[a, b] Kai Sun,[c] and Dean M. Giolando*[a]

This work describes the electrocatalysis of amorphous nickel phosphide (Ni-P) electrodeposited onto copper metal foil, for its use as a non-noble metal catalyst for the hydrogen evolution reaction (HER) in 0.5 M H_2SO_4. Although electrodeposition offers many advantages over conventional high temperature and high pressure fabrication techniques, there are very few reports on the preparation of Ni-P electrocatalysts via electrodeposition. This Ni-P electrocatalyst exhibits good activity in acidic medium, with a potential of −222 mV to achieve 10 mA cm^{-2} cathodic current density. This potential is comparable to that of electrodeposited Pt black (−104 mV), and much better than that of electrodeposited Ni (−480 mV). An unusual long-term stability in acidic medium was demonstrated by the −222 mV potential remaining constant after 5000 cyclic voltammetric sweeps in 0.5 M H_2SO_4. Importantly, the stoichiometry of the nickel phosphide films can be easily varied from an atomic % of phosphorus from 15 % to as high as 24 % by modifications to the electrodeposition conditions. Such a high phosphorous loading is greater than is generally reported with electrodeposited Ni-P materials. In addition, we observed Ni-P films electrodeposited at lower temperatures (~ 3 °C) result in higher phosphorous loading, which gives rise to enhanced stability as well as activity. Electrodeposited amorphous Ni-P can therefore be used as an active, stable and Earth-abundant metal catalyst for the HER in acidic electrolytes.

Introduction

Developing clean and renewable alternatives to fossil fuels is needed due to the rapid depletion of fossil fuels coupled with harmful effects caused to the environment. Solar, wind, and other sources of renewable energy have been considered, yet, the time of the day and/or weather condition can limit their direct use. To overcome these limitations the energy from renewable sources potentially can be stored as chemical bonds in molecules.[1] Dihydrogen (H_2) has been recognized as a good alternate energy carrier, since it has comparatively high specific energy and it is a zero emission fuel with water as the only combustion product.[2] Compared to other methods, water electrolysis is a promising approach to produce H_2, since water is renewable and provides pure H_2.[3] Noble metals, such as platinum are considered the best heterogeneous metal catalysts for the Hydrogen Evolution Reaction (HER), but their scarcity and high cost limit their applicability.[2,4] Thus, developing inexpensive, highly active non-noble catalysts has become a key challenge.[4b] Nickel, its alloys, and its sulfides, selenides and phosphides are well known non-noble HER catalysts.[5] Among them, nickel phosphides (Ni-P) have shown promising catalytic activity for the HER.[3a,4c,5g,6] However, most of the current methods of making Ni-P requires conditions such as high temperatures, high pressures, inert atmospheres, and other conditions adding complexity to the process.[4c,5g,6c,7] In 2015, Ledendecker, et al. showed that nanostructured Ni_5P_4 has a high activity for the HER and also showed Ni_5P_4 to be more active than metallic Ni.[5g] They used a high temperature synthetic method, where a contact-conversion synthesis was carried out; red phosphorus was distributed on a Ni foil and heated at 550 °C. In addition, Laursen, et al. in 2015 synthesized Ni_5P_4 at high temperatures, and the resultant product was pressed into a pellet, which was then attached to the electrode.[4c]

In this report, the simpler method of electrodeposition is investigated to prepare Ni-P alloys exhibiting good activity and stability upon water electrolysis. Electrodeposition provides several benefits compared to other conventional methods of producing thin films of metal catalysts. Electrodeposition is usually carried out under normal laboratory conditions, which does not require high temperatures, vacuum or high pressures. Adjusting the electrochemical parameters can easily control the composition, thickness, quality and morphology of the film. In

[a] R. N. Wasalat hanthri, S. Jeffrey, N. Su, Prof. D. M. Giolando
Department of Chemistry and Biochemistry
School of Green Chemistry and Engineering,
University of Toledo
Toledo, OH, 43606, USA
E-mail: dean.giolando@utoledo.edu
[b] N. Su
Department of Chemical Engineering
University of Toledo
Toledo, OH, 43606, USA
[c] Prof. K. Sun
Department of Materials Science and Engineering
University of Michigan
Ann Arbor, MI, 48109, USA

Supporting information for this article is available on the WWW under https://doi.org/10.1002/slct.201701755

addition, electrodeposition provides relatively uniform coatings, higher deposition rates, better adhesion, and the apparatus is incredibly simple and inexpensive.[8]

Few studies have been performed on electrodeposited Ni-P as a HER catalyst. The research performed by Burchardt, et al. (2001 and 2002) and Jiang, et al. (2016, with an overpotential of –93 mV for Ni-P and ~ 0 mV for Pt to achieve 10 mA cm^{-2} cathodic current density) provides examples, however only the catalytic activity in alkaline medium was reported.[6b,9] The overpotential for water electrolysis in acidic electrolytes is comparatively lower than in alkaline electrolytes, and ultimately provides higher power efficiency. Thus, non-noble metal catalysts stable in acidic electrolytes has received much attention. Conventional non-noble metal catalysts have very low stability in acidic electrolytes. For example, electrodeposited Ni studied as a comparison in this work galvanically reacted in acidic solution showing its very low stability. However, incorporation of some phosphorus in the metal provides enhanced activity and stability. [1, 10] Some properties of metal phosphides have provided insights into their improved stability. Dissolution of metals is thermodynamically less favorable when alloyed with phosphorus, and as metal phosphides usually form amorphous films, they are less prone to be attacked at the grain boundaries.[10a, 11] If the metal phosphide were to undergo oxidation, nickel phosphate is formed, which can act as a diffusion barrier to prevent the dissolution of metal phosphide alloy.[10a, 11]

According to the reported literature, the maximum phosphorus loading that can be achieved from electrodeposition techniques are about 12-15 atomic % of phosphorus (P *at%*), and to the best of our knowledge, there are no published work related to electrodeposited Ni-P as a HER catalyst in acidic medium.[10a] However, we find that, higher P *at%* can be obtained using an electroplating bath with a higher pH (Brenner type electroplating bath)[12] and an increased concentration of the phosphorus precursor, NaH_2PO_2. The traditional electroplating bath for Ni-P is acidic, and the film obtained from this bath (denoted as Ni-P (Acidic Bath)) gives ~ 13 P *at%*.[9-10] By modifying the electroplating bath to alkaline (a Brenner type electroplating bath) and with a few other modifications, it was possible to achieve films with a higher concentration of phosphorus, up to ~ 24 P *at%*. The Ni-P film obtained from Brenner type electroplating bath (denoted as Ni-P (Brenner)) shows a better stability in acidic electrolyte than Ni-P (Acidic Bath). Additionally, we also show that choose of the metal substrate used for electrodeposition of Ni-P is important, since galvanic dissolution of the substrate in acidic electrolytes can occur with concomitant delamination of Ni-P coating from the surface.

Results and Discussion

Composition and Morphology of Ni-P films

Scanning electron microscopic images of both as-deposited films of Ni-P (Brenner) and Ni-P (Acidic Bath) show slight roughness on the surface, but in contrast to the Ni-P (Brenner), the Ni-P (Acidic Bath) shows the presence of many pinholes and some cracking (Figure 1A and 1B), which is also observed

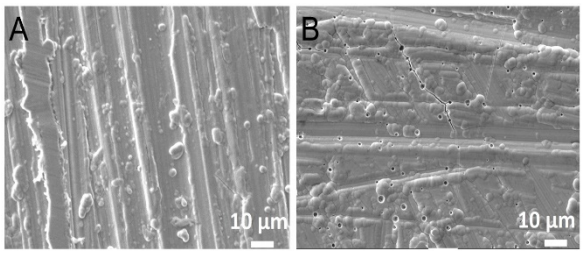

Figure 1. SEM images of as-deposited Ni-P films (A) Ni-P (Brenner), (B) Ni-P (Acidic Bath).

in the literature.[9b] The presence of Ni and P were confirmed by EDX analysis (Supporting Information; Figure S3, S5, S7 and S9), and the quantification resulted a phosphorus content in the as-deposited Ni-P (Brenner) and Ni-P (Acidic Bath) to be ~ 15.5 P *at%* and ~ 13.6 P *at%*, respectively. Elemental mapping by SEM-EDX revealed an even distribution of Ni and P on both electrodeposited Ni-P films (Supporting Information; Figure S4, S6, S8 and S10). The SEM images of the cross sections of Ni-P (Brenner) (Figure S11) and Ni-P (Acidic Bath) (Figure S12) revealed a thickness of ~ 10 µm and ~ 3 µm, respectively. There were no peaks in X-ray diffraction pattern (Figure S13), which indicates the electrodeposited Ni-P films are not crystalline.

Activity and stability of Ni-P towards HER

Polarization plots comparing the HER activity of Ni-P (Brenner) and Ni-P (Acidic Bath) to electrodeposited Pt black, commercial Ni_2P powder and Ni in 0.5 M H_2SO_4 with 5 mV s^{-1} scan rate are collected in Figure 2A and 2B. Both types of Ni-Ps show activities higher than to both Ni_2P and electrodeposited metallic Ni coating on Cu substrates (Ni (Watts)). The potential (not *iR* corrected) required to achieve 10 mA cm^{-2} cathodic current density were –104 mV, –216 mV, –250 mV, –294 mV and –480 mV for electrodeposited Pt black, Ni-P (Acidic Bath), Ni-P (Brenner), Ni_2P and Ni (Watts), respectively. These potentials for all the catalysts reported in our work are relatively higher compared to most literature reported data. This is due to the difference in the electrode set up used in this work (which is different than the usual rotating disk electrodes), and the measurements were obtained under diffusion controlled system. Thus comparing these overpotentials to other reported values is difficult, however a comparison to a more active standard of Pt under the same conditions, would still provide a good evaluation of the catalysts. In addition, the current densities reported in this work are based on the geometrical surface area, which can be different than the electroactive surface area. Electroactive surface area can be either higher or lower compared to the geometrical surface area, depending on the surface morphology of the electrode and the electrochemical reaction occurring on the electrode surface. In HER experiments, we observed some bubbles adhering to the

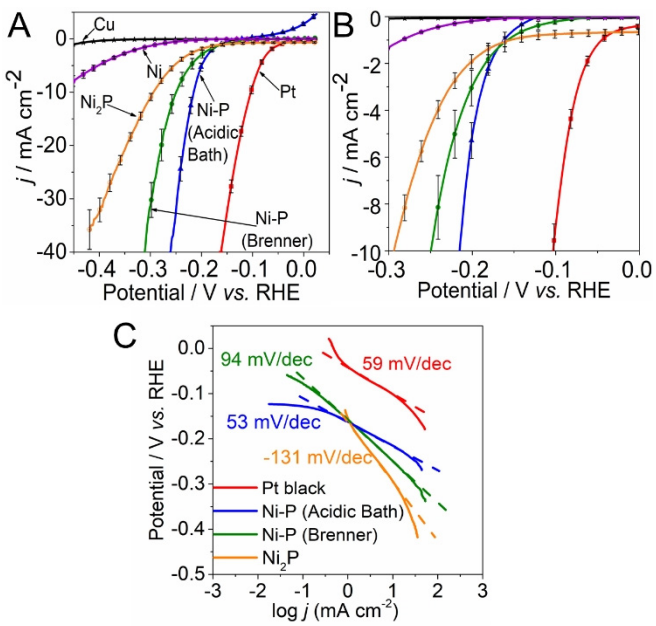

Figure 2. (A) Polarization data and (B) an inset of the polarization curves for electrodeposited Pt black (red), Ni-P (Acidic Bath) (blue), Ni-P (Brenner) (green), commercial Ni_2P (orange) Ni (Watts) (purple) films and blank copper foil (black) in 0.5 M H_2SO_4; scan rate is 5 mV s^{-1}. The inset shows the polarization data at the initial stage (from 0 V to –0.3 V vs RHE) of the electrolysis. The values represent the mean ± standard deviation (SD) based on 3 independent experiments. (C) Corresponding Tafel plots (with linearly fitted dashed lines) derived from the polarization curves.

electrode surface. This reduces the available active surface area for the HER and thus, we believe the actual current densities might be higher than the observed current densities. However, the initial stages of the HER prior to the formation of bubbles can be used to compare the activity of the different electrode coatings. The corresponding Tafel plots (Figure 2C) were obtained and the linear portions were fitted to the Tafel equation ($\eta = b \log |j| + a$, where j is the current density and b is the Tafel slope), which yielded Tafel slopes of 59 mV dec^{-1}, 53 mV dec^{-1}, 94 mV dec^{-1} and 131 mV dec^{-1} for Pt black, Ni-P (Acidic Bath), Ni-P (Brenner), and commercial Ni_2P, respectively. Tafel slope and the exchange current density (j_0) are two important parameters that reflect the intrinsic activity and the mechanism on different electrodes. Small Tafel slope and higher j_0 are indicative of more favorable HER catalytic activity. Exchange current density can be obtained by extracting the current density at 0 V vs RHE, and higher j_0 represents a higher electron transfer or proton adsorption/desorption at the electrode surface with a lower kinetic barrier. In this work, the Tafel slope for Pt black does not match with the values that are generally reported with Pt/C electrodes (~ 30 mv dec^{-1}), which can be attributed by the difference in mechanism and activity on different types of Pt electrodes.[1] The commericial Ni_2P powder resulted a tafel slope of 131 mV dec^{-1}, which is comparable with previously reported data.[10a] Tafel slopes of 59 mV dec^{-1} and 53 mV dec^{-1} indicate the Volmer-Heyrovski type mechanism for HER on Pt black and Ni-P (Acidic Bath), with Heyrovski step (desorption step: $H_{ads} + H_3O^+ + e^- \leftrightarrows H_2 + H_2O$) as the slow step. The Tafel slope of 94 mV dec^{-1} and 131 mV dec^{-1} for Ni-P (Brenner) and commercial Ni_2P, respectively, indicate a Volmer-Tafel type mechanism with slow Volmer step (discharge step: $H_3O^+ + e^- \leftrightarrows H_{ads} + H_2O$). The observed j_0 for Pt black, Ni-P (Acidic Bath), Ni-P (Brenner) and Ni_2P are 0.72 mA cm^{-2}, 3.2 mA cm^{-2}, 1.6 mA cm^{-2} and 1.2 mA cm^{-2}, respectively. The j_0 values for both Ni-Ps are greater compared to some recently reported Ni-P HER catalysts,[3a,4a,10a] indicating their higher performance towards HER in acidic medium.

The cyclic voltammograms of Ni-P (Brenner) (Figure S14) shows a current only due to the irreversible reduction of H^+ to H_2, and no additional peaks are present. This implies no other electrochemical reaction occurs during the electrolysis except the HER. Comparison of the Faradaic yield for H_2 production on Ni-P (Brenner) films is contained in Figure 3, and the quantitative H_2 production is agreeable within experimental errors.

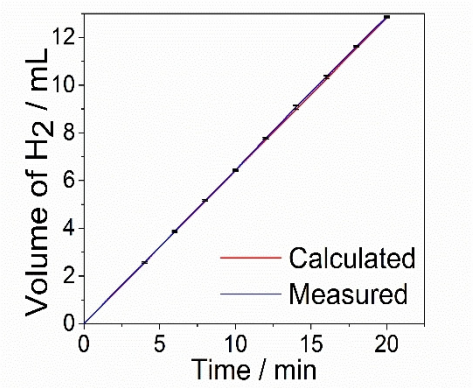

Figure 3. Volume of H_2 generated on Ni-P (Brenner) films when a current of 85.4 mA is passed over 20 minutes in 0.5 M H_2SO_4 versus calculated quantities assuming 100% Faradaic efficiency for the HER. The values represent the mean ± SD based on 3 independent experiments.

The stability of films prepared from the Ni-P (Brenner) solution was compared to films prepared from the Ni-P (Acidic Bath) solution, by examining the polarization plots of the as-deposited films and after undergoing 5000 cyclic voltammetric sweeps (from –150 mV to –500 mV *vs* Ag/AgCl (3 M NaCl)) in 0.5 M H_2SO_4, which is indicated in Figure 4A. Even though Ni-P (Acidic Bath) has a better activity, Ni-P (Brenner) shows better stability in acidic electrolyte. The change in activity in Ni-P (Brenner) is fairly small. The potential for 10 mA cm^{-2} cathodic current density increased only by ~ 14 mV in Ni-P (Brenner), while in Ni-P (Acidic Bath) the potential increased by ~ 59 mV. Initially, the Ni-P (Acidic Bath) exhibits an anodic current from 0 to ~ 0.1 V, which has been observed by others and has been suggested to be due to oxidation of the Ni-P, but after 5000 CV sweeps no current is observed until the onset of electrolysis at ~ 0.15 V.[13] Nickel phosphide (Acidic Bath) film contains many pin holes and cracks as can be observed in Figure 1B, which increases the available surface area for electrolysis. Thus, the higher current density observed in Ni-P (Acidic Bath) could be

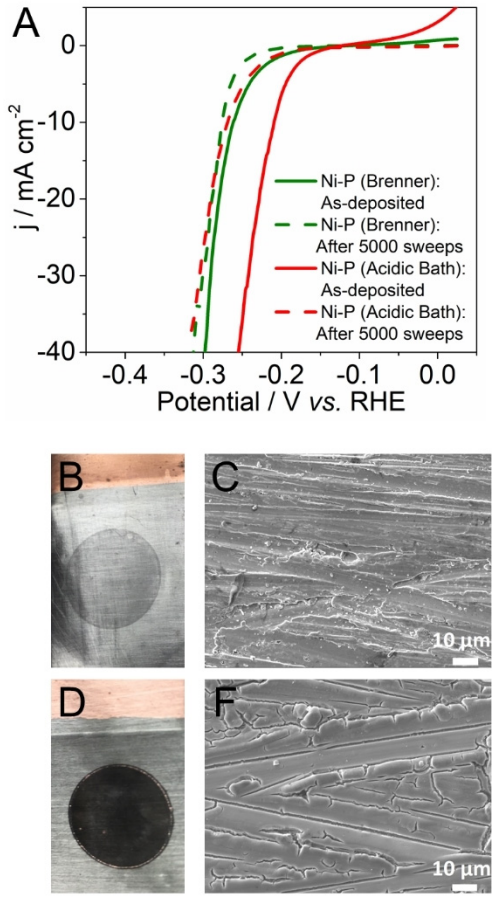

Figure 4. A) Polarization data comparing the stability of Ni-P (Brenner) (green) and Ni-P (Acidic Bath) (red) films in 0.5 M H_2SO_4 (solid lines: as-deposited films, dotted lines: after 5000 cyclic voltammetry sweeps); scan rate is 5 mV s^{-1}. Long term stability was analyzed by comparing the activity of Ni-P films before and after 5000 cyclic voltammetric sweeps (from −150 mV to −500 mV vs Ag/AgCl (3 M NaCl)) in 0.5 M H_2SO_4 at a scan rate of 100 mV s^{-1}, (B, D) images of (B) Ni-P (Brenner) and (D) Ni-P (Acidic Bath) films comparing before and after 5000 cyclic voltammetric sweeps, (C, E) SEM images of (C) Ni-P (Brenner) and (E) Ni-P (Acidic Bath) films after 5000 cyclic voltammetric sweeps.

partly attributed by the increased surface area as well. The change in the morphology of both films before and after 5000 cyclic voltammetric sweeps is shown in the images in Figure 4B and 4D. The circular area inside the film represents the coated area that underwent electrolysis, and the area outside of the circle is the as-deposited film. After running 5000 cyclic voltammetric sweeps, Ni-P (Acidic Bath) appears more corroded than Ni-P (Brenner). Scanning electron microscopy images of the Ni-P (Brenner) (Figure 4C) possess a smoothing of the surface compared to the as-deposited film (Figure 1A), and there are neither cracks nor pinholes, whereas in Ni-P (Acidic Bath) (Figure 4E) there are enhanced cracks in comparison to Figure 1B. A common feature observed for both films was that the P *at%* increased after electrolysis. Quantification from EDX showed that P *at%* was ~ 26.5% and ~ 33.1% in Ni-P (Brenner) and Ni-P (Acidic Bath), respectively, after 5000 cyclic voltammetric sweeps. Increase in P content implies that during the electrolysis some of the Ni is removed from the film, probably as galvanic dissolution in acidic medium. However, this effect is less in Ni-P (Brenner), as indicated by the lower increment of P *at%*. The amounts of Ni leached into the eletrolyte during the long term electrolysis were further analyzed by atomic absorption spectroscopy (AAS) using the method of standard additions. (A detailed description can be found in the supporting information). This AAS analysis provides a good approximation of the amount of Ni leached during the electrolysis. The total mass of Ni dissolved in the electrolyte were found to be ~ 80 µg and ~ 240 µg (on a surafce area of 1.33 cm^2) for Ni-P (Brenner) (Figure S15A) and Ni-P (Acidic Bath) (Figure S15B), respectively, after the 5000 cyclic voltammetric sweeps in 0.5 M H_2SO_4. These results validate the lower Ni dissolution in Ni-P (Brenner) compared to Ni-P (Acidic Bath).

XPS analysis of as-deposited and post HER Ni-P films

The chemical states of the Ni and P on the surfaces of Ni-P films were characterized by XPS. Figure 5A to 5H show the XPS spectra of the Ni 2p and P 2p regions for as-deposited Ni-P (Brenner), Ni-P (Brenner) after 5000 cyclic voltammetric sweeps in 0.5 M H_2SO_4, Ni-P (Acidic Bath) and Ni-P (Acidic Bath) after 5000 cyclic voltammetric sweeps in 0.5 M H_2SO_4, respectively. A complete peak assignment of the XPS spectra can be found in the Supporting Information (Table S2). All of the four films display the presence of two types of Ni centers and two types of P centers. The peaks at 852.8 eV in Figure 5A and 852.9 eV in Figure 5E are assigned to Ni $2p_{3/2}$ binding energy of $Ni^{\delta+}$ in as-deposited Ni-P (Brenner) film and as-deposited Ni-P (Acidic Bath), respectively. These values are higher than the values observed for zero valance Ni (852.4 - 852.6 eV) and are comparable with the values reported in the literature for $Ni^{\delta+}$ in Ni-P.[14] The peaks at 129.4 eV in Figure 5B and 5F are assigned to P $2p_{3/2}$ binding energy of $P^{\delta-}$ in Ni-P in as-deposited Ni-P (Brenner) and as-deposited Ni-P (Acidic Bath), respectively. This value is lower than that of elemental P (130.2 eV), and implies the presence of a small negative charge on P.[14a, d] After 5000 cyclic voltammetric sweeps in 0.5 M H_2SO_4, peaks at 853.2 eV in Figure 5C and 853.4 eV in Figure 5G are assigned to Ni $2p_{3/2}$ binding energy of $Ni^{\delta+}$ in Ni-P (Brenner) film and Ni-P (Acidic Bath) film, respectively. The peaks for P $2p_{3/2}$ binding energy of $P^{\delta-}$ for Ni-P (Brenner) and Ni-P (Acidic Bath) after 5000 cyclic voltammetric sweeps appear at 129.3 eV in Figure 5D and 5H, respectively. A closer examination of the binding energies of both Ni-P films showed a change in the binding energy from as-deposited films to the films that underwent 5000 cyclic voltammetric sweeps. These changes are summarized in Table 1 and shows a considerable increase in the positive charge on the $Ni^{\delta+}$ centers. This could be caused by the galvanic dissolution of Ni during the electrolysis that lowers the amount of Ni on the film. A reduction in the amount of Ni results in a higher positive charge on the Ni centers to compensate the increased negative charge due to the greater amount of P in the Ni-P films. The EDX quantification of the Ni-P films after 5000 cyclic voltammetric sweeps showed higher Ni loss in Ni-P (Acidic Bath) (indicated in Table 1) and that explains

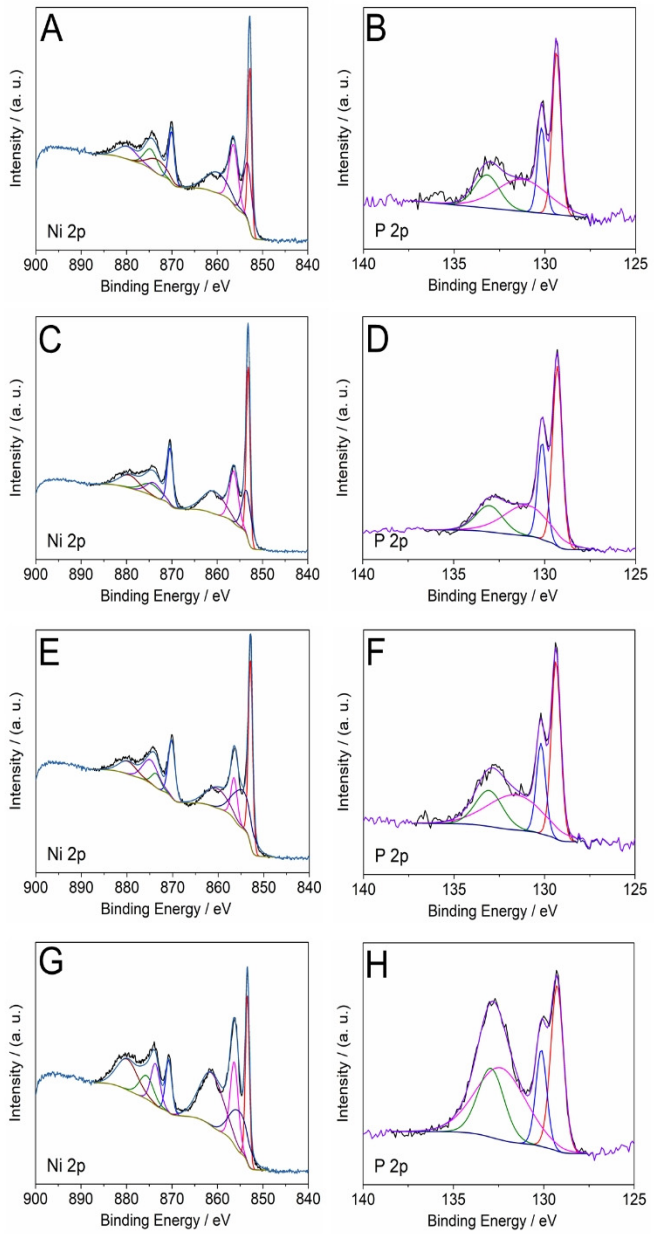

Figure 5. XPS spectra of the Ni 2p and P 2p regions for (A and B) as-deposited Ni-P (Brenner), (C and D), Ni-P (Brenner) after 5000 cyclic voltammetric sweeps in 0.5 M H_2SO_4, (E and F) as-deposited Ni-P (Acidic Bath), (G and H), Ni-P (Acidic Bath) after 5000 cyclic voltammetric sweeps in 0.5 M H_2SO_4.

the higher increase in $Ni^{\delta+}$ binding energy of Ni-P (Acidic Bath) compared to that of Ni-P (Brenner). In addition to Ni-P peaks, peaks due to oxidized Ni and oxidized P also appear in the XPS spectra of all four films. Oxidized Ni and P species are formed

Table 1. Binding energy shift in Ni $2P_{3/2}$ and P $2p_{3/2}$ energy levels, change in Ni *at%* and P *at%*, from as-deposited films to those after 5000 cyclic voltammetric sweeps in 0.5 M H_2SO_4.

	Ni-P (Brenner)	Ni-P (Acidic Bath)
ΔBE $Ni^{\delta+}$/eV[a]	+0.36	+0.49
ΔBE $P^{\delta-}$/eV[a]	−0.06	−0.10
$\triangle$Ni *at%*	−11.0	−19.5
$\triangle$P *at%*	+11.0	+19.5

[a] BE stands for binding energy.

due to the surface passivation, since the samples are exposed to air. The peaks at 856.4 eV in Figure 5A and 856.5 eV in Figure 5E are attributed to Ni $2p_{3/2}$ binding energy of oxidized Ni of nickel phosphate on the Ni-P surfaces of as-deposited Ni-P (Brenner) and as-deposited Ni-P (Acidic bath), respectively. Moreover, the peaks at 131.2 eV in Figure 5B and 131.6 eV in Figure 5F correspond to the P $2p_{3/2}$ binding energy of oxidized P in as-deposited Ni-P (Brenner) and as-deposited Ni-P (Acidic bath), respectively. After 5000 cyclic voltammetric sweeps in 0.5 M H_2SO_4, peaks at 856.3 eV in Figure 5C and 5G are assigned to Ni $2p_{3/2}$ binding energy of oxidized Ni in Ni-P (Brenner) film and Ni-P (Acidic bath) film, respectively. The peaks for P $2p_{3/2}$ binding energy of oxidized P for Ni-P (Brenner) and Ni-P (Acidic bath) after 5000 cyclic voltammetric sweeps appear at 131.0 eV in Figure 5D and 132.4 eV in Figure 5H, respectively.

Effect of electrodeposition current density, temperature and concentration of NaH_2PO_2 in the bath on HER activity

The effects of deposition current density and temperature were investigated for Ni-P (Brenner) solutions. The polarization plot in Figure 6 compares the activity of the Ni-P (Brenner) films

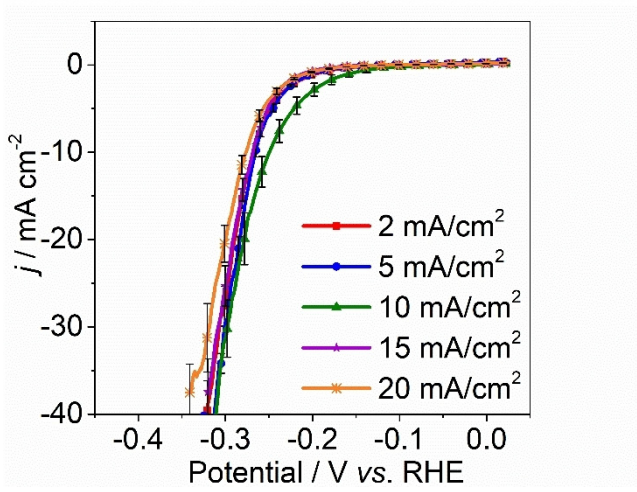

Figure 6. Polarization data in 0.5 M H_2SO_4 for Ni-P (Brenner) films electro-deposited at different current densities of 2 mA cm^2 (red), 5 mA cm^{-2} (blur), 10 mA cm^{-2} (green), 15 mA cm^{-2} (purple) and 20 mA cm^{-2} (orange); scan rate is 5 mV s^{-1}. The values represent the mean ± SD based on 3 independent experiments.

made using different deposition current densities (at room temperature: 21 ± 1 °C). A slight difference in activity can be observed depending on the current density used for electrodeposition, and average current density of 10 mA cm^{-2} provides a better activity compared to the films made at lower current densities (2-5 mA cm^{-2}) and higher current densities (15-20 mA cm^{-2}). Atomic % of P of these films (from EDX) were ~ 16.6%, 15.7%, 15.5%, 15.6% and 15.7% for the Ni-P (Brenner) films made using current densities of 2 mA cm^2, 5 mA cm^{-2}, 10 mA cm^{-2}, 15 mA cm^{-2} and 20 mA cm^{-2}, respectively, indicating there is no significant effect to the P *at%* in the films due to the changes in electrodeposition current density. This might also be the reason for observing only a slight change in activity as well. The slightly lower activity of the films made at high current densities might be explained based by high current densities causing fast nucleation, which could result in lower quality films.

In contrast to changes in deposition current density, a notable change in the activity of Ni-P (Brenner) films could be observed based on the temperature of the bath used during electrodeposition, as indicated in Figure 7A. Films prepared at lower temperatures give the best activity, while the films prepared at higher temperatures give very low activity. The activity of the films decreased based on the deposition temperature in the order of 3 °C > 10 °C > 21 °C > 50 °C > 75 °C. The potential required to achieve 10 mA cm^{-2} cathodic current density were –235 mV, –250 mV, –250 mV, –393 mV and –429 mV for the Ni-P (Brenner) films prepared at deposition temperatures of 3 °C, 10 °C, 21 °C, 50 °C and 75 °C, respectively. Although the Ni-P (Brenner) films prepared at 10 °C and 21 °C have the same potential to achieve 10 mA cm^{-2} cathodic current density, an enhanced current rise can be observed beyond –250 mV in the films made at 10 °C.

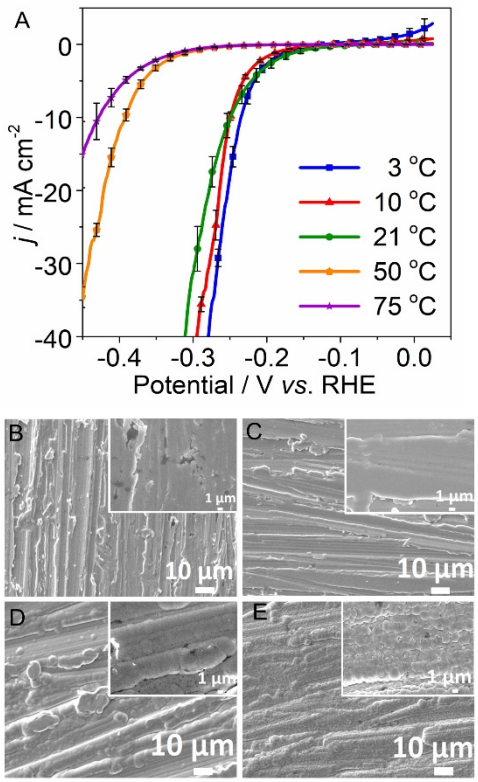

Figure 7. (A) Polarization data in 0.5 M H_2SO_4 for Ni-P (Brenner) films electrodeposited at different temperatures of 3 °C (blue), 10 °C (red), 21 °C (green), 50 °C (orange) and 75 °C (purple); scan rate is 5 mV s^{-1}. The values represent the mean ± SD based on 3 independent experiments. (B-E) SEM images of Ni-P (Brenner) films electrodeposited at varied temperatures of (B) 3 °C, (C) 10 °C, (D) 50 °C, (E) 75 °C. The insets are further zoomed in SEM images.

Attempts were taken to prepare Ni-P (Brenner) films at –5 °C and –10 °C, however the electrodepositions were inhibited by the precipitation of the salts in the electroplating bath. We could also observe that the P content in the film is notably affected by the temperature used for electrodeposition. The P *at%* were 24.0%, 22.7%, 15.5%, 13.9% and 12.3% for the films deposited at temperatures of 3 °C, 10 °C, 21 °C, 50 °C and 75 °C, respectively, indicating the use of lower temperatures results in higher amount of phosphorus in the film. Higher activity of the Ni-P (Brenner) films deposited at lower temperatures could also be due to the presence of higher P content. Increasing the deposition temperature seems to lower the P content in the film. Surface morphology of the films prepared at higher temperatures were also slightly different than that prepared at lower temperatures, as indicated by Figure 7B to 7E and in the Supporting Information (Figure S16), where they appear to be less lustrous. In addition, increasing deposition temperature appears to cause a growth of smaller grains of Ni-P. This might be due to higher nucleation rates and thus the availability of more nucleation sites at elevated temperatures.

According to the literature, electrodeposition techniques for Ni-P compounds give a maximum phosphorus loading only up to about 12 – 15 P *at%*.[10a] However, as indicated above, we observe that by low temperature electrodeposition, it is possible to achieve enhanced P *at%* into the films. In addition, we could also observe that by increasing the concentration of NaH_2PO_2 in the Brenner type plating bath and using the normal electrodeposition conditions, it is possible to obtain a phosphorus loading up to about 24 P *at%*. Nickel phosphide films were prepared by increasing the amount of NaH_2PO_2 to 20 g/L, 30 g/L, 40 g/L and 50 g/L in Brenner plating bath, and are named as Ni-P (Brenner: NaH_2PO_2: X g/L), where X denotes the concentration of NaH_2PO_2 in g/L, From the EDX analysis, the average P *at%* of the films made from the plating baths Ni-P (Brenner: 20 g/L NaH_2PO_2), Ni-P (Brenner: 30 g/L NaH_2PO_2), Ni-P (Brenner: 40 g/L NaH_2PO_2) and Ni-P (Brenner: 50 g/L NaH_2PO_2) were ~ 20.2%, 23.8%, 22.4% and 23.7%, respectively. The HER activity of these films was investigated (Figure 8) to determine the effect of phosphorus content. All four Ni-P samples prepared show enhanced activity compared to Ni-P (Brenner). The potential required to achieve 10 mA cm^{-2} cathodic current density were –250 mV, –237 mV, –231 mV, –232 mV and –226 mV for Ni-P (Brenner), Ni-P (Brenner: 20 g/L NaH_2PO_2), Ni-P (Brenner: 30 g/L NaH_2PO_2), Ni-P (Brenner: 40 g/L NaH_2PO_2), and Ni-P (Brenner: 50 g/L NaH_2PO_2), respectively.

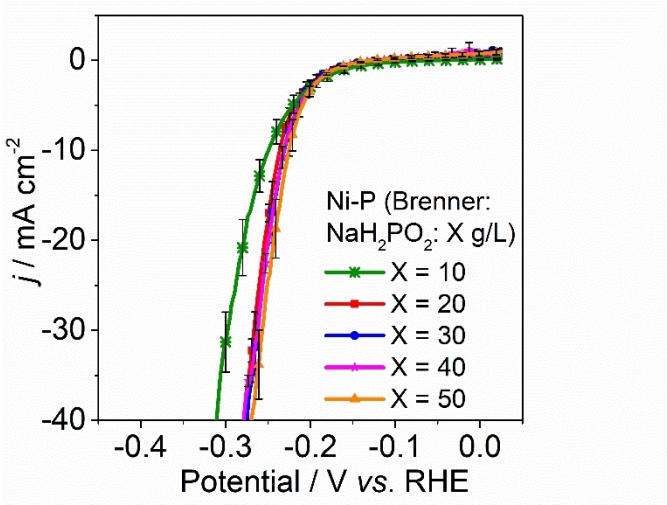

Figure 8. Polarization data in 0.5 M H_2SO_4 for Ni-P (Brenner) films electrodeposited with varied concentration of NaH_2PO_2 in the plating bath. Ni-P (Brenner: X g/L): (X = 10 (green), 20 (red), 30 (blue), 40 (pink) and 50 (orange)); scan rate is 5 mV s^{-1}. The values represent the mean ± SD based on 3 independent experiments.

The activities of optimized Ni-P (Brenner) (denoted as Ni-P (Brenner: Opt.)) and optimized Ni-P (Acidic-bath) (denoted as Ni-P (Acidic Bath: Opt.)) films were compared to that of the respective original films (Figure 9). These optimized films were

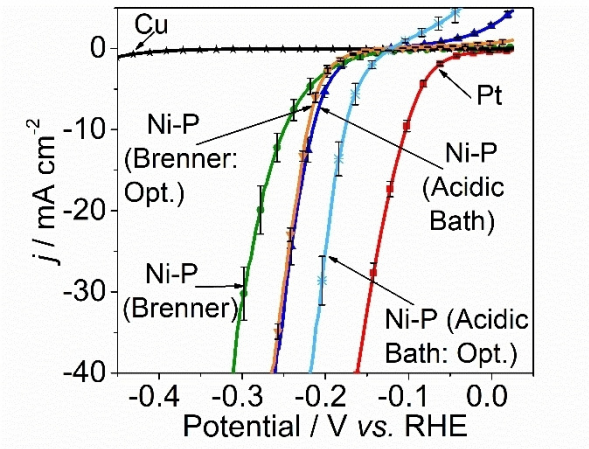

Figure 9. Polarization data for electrodeposited Pt (red), Ni-P (Brenner) (green), Ni-P (Brenner: Opt.) (orange), Ni-P (Acidic Bath) (blue), Ni-P (Acidic Bath: Opt.) (pale blue), films and copper foil (black) in 0.5 M H_2SO_4; scan rate is 5 mV s^{-1}. The values represent the mean ± SD based on 3 independent experiments. .

prepared using the conditions that gave best activity for each parameter tested (i.e. 50 g/L NaH_2PO_2 in the plating bath, electrodeposited at 3 °C using 10 mA cm^{-2} current density). The use of optimized conditions substantially increases the activity of both Ni-P (Brenner) and Ni-P (Acidic bath) films. The potential to achieve 10 mA cm^{-2} cathodic current density was –177 mV and –222 mV for Ni-P (Acidic Bath: Opt.) and Ni-P (Brenner: Opt.), respectively. Compared to the original films, the potential has decreased by 39 mV in Ni-P (Acidic Bath: Opt.) and by 28 mV in Ni-P (Brenner: Opt.). The ~ P *at%* were found to be 24.7% and 16.1% for Ni-P (Brenner: Opt.) and Ni-P (Acidic Bath: Opt.), respectively. This indicates the use of higher concentration of the phosphorous precursor (NaH_2PO_2) in the bath coupled with low temperature deposition can elevate the phosphorus content on the film, and ultimately resulting enhanced activity.

Most of the electrodepositions of Ni-P coatings reported in the literature are performed on either Ni foil or on stainless steel.[9, 11] However, electrodeposited Ni-P onto stainless steel is unstable during electrolysis in 0.5 M H_2SO_4. Initially, it was observed that after ~ 2 h of electrolysis, the Ni-P coating delaminated from the substrate, but this was not observed in alkaline medium. The absence of Ni and P on the stainless steel was confirmed by EDX (Supporting Information: Figure S17A and S12B). Based on this observation, it is possible to conclude that electrodeposited Ni-P onto stainless steel substrate does not have long-term stability in acidic medium. However, this may be due to the stainless steel substrate being galvanically dissolved in acidic medium, thus causing the degradation of the stainless steel substrate. This leads to the delamination of the Ni-P coating. This might be due to the presence of very small pores in the electrodeposited Ni-P that would allow the acidic electrolyte to pass through. Even though these holes are not visible in the SEM images of Ni-P (Brenner), pinholes can be observed in SEM images of Ni-P (Acidic Bath). The reaction of stainless steel with H_2SO_4 is expected, since the reducing potential of Fe is larger than that of H^+ (considering the electrochemical series). Knowing this, we chose to use a metal with a lower reducing potential than that of H^+, such as Cu, as the substrate for electrodepositions of Ni-Ps, which allows investigation of the stability of Ni-P films.

Conclusions

We report electrodeposited Ni-P films can act as highly active and stable electrocatalysts for the HER in acidic electrolytes, with ~100% Faradaic efficiency. Electrodeposited Ni-P films from a Brenner type plating bath required a potential of –222 mV (without *iR* correction) to achieve 10 mA cm^{-2} cathodic current density with a minimal increase in potential after 5000 cyclic voltammetric sweeps. Furthermore, we showed that the amount of P in the film can be increased up to ~ 24 *at%* with modifications to the electrodeposition conditions, such as, higher concentration of the phosphorous precursor (NaH_2PO_2) in the bath and low temperature deposition, which results in increasing the activity. This beneficial effect, accompanied by the simplicity of the film preparation method shows the potential that Earth-abundant Ni-P catalysts hold towards efficient H_2 generation via water splitting.

Supporting Information Summary

Detailed experimental procedures and additional experimental data can be found in the Supporting Information.

Acknowledgements

We greatly acknowledge the support from Dr. Jon R. Kirchhoff (University of Toledo, USA) for sharing electrochemical resources. We are grateful to Mr. Steven D. Moder (University of Toledo, USA) for his valuable skills in glassblowing and for assembling custom glassware for the fulfilment of this research. We also acknowledge the support of the University of Michigan College of Engineering and NSF grant #DMR-0420785 for XPS analysis.

Conflict of Interest

The authors declare no conflict of interest.

Keywords: acid stable nickel phosphide · electrocatalyst · electrodeposition · hydrogen evolution reaction

[1] J. F. Callejas, C. G. Read, C. W. Roske, N. S. Lewis, R. E. Schaak, *Chem. Mater.* **2016**, *28*, 6017-6044.
[2] X. Zou, Y. Zhang, *Chem. Soc. Rev.* **2015**, *44*, 5148-5180.
[3] a) J. Li, J. Li, X. Zhou, Z. Xia, W. Gao, Y. Ma, Y. Qu, *ACS Appl. Mater. Interfaces* **2016**, *8*, 10826-10834; b) N. Bai, Q. Li, D. Mao, D. Li, H. Dong, *ACS Applied Materials & Interfaces* **2016**, *8*, 29400-29407.
[4] a) E. J. Popczun, J. R. McKone, C. G. Read, A. J. Biacchi, A. M. Wiltrout, N. S. Lewis, R. E. Schaak, *J. Am. Chem. Soc.* **2013**, *135*, 9267-9270; b) P. Xiao, M. A. Sk, L. Thia, X. Ge, R. J. Lim, J.-Y. Wang, K. H. Lim, X. Wang, *Energy Environ. Sci.* **2014**, *7*, 2624-2629; c) A. B. Laursen, K. R. Patraju, M. J. Whitaker, M. Retuerto, T. Sarkar, N. Yao, K. V. Ramanujachary, M. Greenblatt, G. C. Dismukes, *Energy Environ. Sci.* **2015**, *8*, 1027-1034; d) M. A. Abbas, J. H. Bang, *Chem. Mater.* **2015**, *27*, 7218-7235.
[5] a) Z. Xie, P. He, L. Du, F. Dong, K. Dai, T. Zhang, *Electrochim. Acta* **2013**, *88*, 390-394; b) K. Ngamlerdpokin, N. Tantavichet, *Int. J. Hydrogen Energy* **2014**, *39*, 2505-2515; c) C. Lupi, A. Dell'Era, M. Pasquali, *Int. J. Hydrogen Energy* **2009**, *34*, 2101-2106; d) P. Ragunathan, S. K. Mitra, M. G. Nayar, *Int. J. Hydrogen Energy* **1981**, *6*, 487-496; e) N. Jiang, L. Bogoev, M. Popova, S. Gul, J. Yano, Y. Sun, *J. Mater. Chem. A* **2014**, *2*, 19407-19414; f) M.-R. Gao, Z.-Y. Lin, T.-T. Zhuang, J. Jiang, Y.-F. Xu, Y.-R. Zheng, S.-H. Yu, *J. Mater. Chem.* **2012**, *22*, 13662-13668; g) M. Ledendecker, S. Krick Calderón, C. Papp, H.-P. Steinrück, M. Antonietti, M. Shalom, *Angew. Chem. Int. Ed.* **2015**, *54*, 12361-12365; *Angew. Chem.* **2015**, *127*, 12538–12542; h) X. Zhou, Y. Liu, H. Ju, B. Pan, J. Zhu, T. Ding, C. Wang, Q. Yang, *Chem. Mater.* **2016**, *28*, 1838-1846; i) D. Li, K. Senevirathne, L. Aquilina, S. L. Brock, *Inorg. Chem.* **2015**, *54*, 7968-7975.
[6] a) L. Feng, H. Vrubel, M. Bensimon, X. Hu, *PCCP* **2014**, *16*, 5917-5921; b) N. Jiang, B. You, M. Sheng, Y. Sun, *ChemCatChem* **2016**, *8*, 106-112; c) A. Han, S. Jin, H. Chen, H. Ji, Z. Sun, P. Du, *J. Mater. Chem. A* **2015**, *3*, 1941-1946; d) Y. Pan, Y. Chen, Y. Lin, P. Cui, K. Sun, Y. Liu, C. Liu, *J. Mater. Chem. A* **2016**, *4*, 14675-14686.
[7] X. Wang, Y. V. Kolen'ko, X.-Q. Bao, K. Kovnir, L. Liu, *Angew. Chem. Int. Ed.* **2015**, *54*, 8188-8192; *Angew. Chem.* **2015**, *127*, 8306–8310.
[8] I. Dharmadasa, J. Haigh, *J. Electrochem. Soc.* **2006**, *153*, G47-G52.
[9] a) T. Burchardt, *Int. J. Hydrogen Energy* **2002**, *27*, 323-328; b) T. Burchardt, V. Hansen, T. Våland, *Electrochim. Acta* **2001**, *46*, 2761-2766.
[10] a) A. R. J. Kucernak, V. N. Naranammalpuram Sundaram, *J. Mater. Chem. A* **2014**, *2*, 17435-17445; b) M. V. Gerasimov, Y. N. Simirskii, *Metallurgist* **2008**, *52*, 477-481.
[11] B. Elsener, M. Crobu, M. A. Scorciapino, A. Rossi, *J. Appl. Electrochem.* **2008**, *38*, 1053.
[12] A. Brenner, G. E. Riddell, *J. Res. NBS* **1946**, *37*, 31-34.
[13] L. Jin, H. Xia, Z. Huang, C. Lv, J. Wang, M. G. Humphrey, C. Zhang, *J. Mater. Chem. A* **2016**, *4*, 10925-10932.
[14] a) Y. Pan, Y. Liu, J. Zhao, K. Yang, J. Liang, D. Liu, W. Hu, D. Liu, Y. Liu, C. Liu, *J. Mater. Chem. A* **2015**, *3*, 1656-1665; b) M. C. Biesinger, B. P. Payne, L. W. Lau, A. Gerson, R. S. C. Smart, *Surf. Interface Anal.* **2009**, *41*, 324-332; c) P. W. Menezes, A. Indra, C. Das, C. Walter, C. Göbel, V. Gutkin, D. Schmeiβer, M. Driess, *ACS Catal.* **2016**, 103-109; d) J. A. Cecilia, A. Infantes-Molina, E. Rodríguez-Castellón, A. Jiménez-López, *J. Catal.* **2009**, *263*, 4-15.

Submitted: August 2, 2017
Accepted: September 4, 2017